The Astrophysical Journal, 648:1206–1218, 2006 September 10

ACCRETION DISKS AROUND YOUNG STARS: LIFETIMES, DISK LOCKING, AND VARIABILITY

Ray Jayawardhana, Jaime Coffey, Alexander Scholz, Alexis Brandeker, and Marten H. van Kerkwijk
Department of Astronomy and Astrophysics, University of Toronto, Toronto, ON M5S 3H8, Canada; rayjay@astro.utoronto.ca
Received 2005 November 11; accepted 2006 May 23

ABSTRACT

We report the findings of a comprehensive study of disk accretion and related phenomena in four of the nearest young stellar associations spanning 6–30 million years in age, an epoch that may coincide with the late stages of planet formation. We have obtained ∼650 multiepoch high-resolution optical spectra of 100 low-mass stars that are likely members of the η Chamaeleontis (∼6 Myr), TW Hydrae (∼8 Myr), β Pictoris (∼12 Myr), and Tucanae-Horologium (∼30 Myr) groups. Our data were collected over 12 nights between 2004 December and 2005 July on the Magellan Clay 6.5 m telescope. Based on Hα line profiles, along with a variety of other emission lines, we find clear evidence of ongoing accretion in 3 out of 11 η Cha stars and 2 out of 32 TW Hydrae members. None of the 57 β Pic or Tuc-Hor members shows measurable signs of accretion. Together, these results imply significant evolution of the disk-accretion process within the first several Myr of a low-mass star's life. While a few disks can continue to accrete for up to ∼10 Myr, our findings suggest that disks accreting for beyond that timescale are rather rare. This result provides an indirect constraint on the timescale for gas dissipation in inner disks and, in turn, on gas-giant planet formation. All accretors in our sample are slow rotators, whereas nonaccretors cover a large range in rotational velocities. This may hint at rotational braking by disks at ages up to ∼8 Myr. Our multiepoch spectra confirm that emission-line variability is common even in somewhat older T Tauri stars, among which accretors tend to show particularly strong variations. Thus, our results indicate that accretion and wind activity undergo significant and sustained variations throughout the lifetime of accretion disks.

Subject headings: accretion, accretion disks — circumstellar matter — open clusters and associations: individual (η Chamaeleontis, TW Hydrae, β Pictoris, Tucanae-Horologium) — planetary systems — stars: formation — stars: low-mass, brown dwarfs

1. INTRODUCTION

Since planets are born in circumstellar disks, studies of disk evolution can provide useful constraints on the timescale for planet formation. The recently identified young stellar associations, located within 100 pc of the Sun and spanning the critical age range of ∼5–30 Myr, constitute superb targets for such investigations. The growing consensus, primarily from infrared observations of these groups and other young clusters, is that (at least) the inner disks are cleared of small dust grains within the first 6–10 Myr (e.g., Haisch et al. 2001, 2005; Jayawardhana et al. 1999b). Unfortunately, little is known about the timescale for the dissipation of gas, which accounts for ∼99% of the disk mass and is crucial for building giant planets. That is because cold molecular gas, especially H_2, is hard to detect (e.g., Richter et al. 2002). It is possible to determine the presence of gas in the inner disk, albeit indirectly, from evidence of gas being accreted from the inner disk edge onto the central star. Perhaps the most readily seen signature of infalling gas in low-mass stars and brown dwarfs is a broad, asymmetric and, usually, strong Hα emission line, although other diagnostic lines have also been identified (e.g., Muzerolle et al. 2001; Jayawardhana et al. 2003). The presence or absence of accretion signatures thus provides a valuable probe of inner disk evolution. By comparing the fraction of objects with signs of ongoing accretion in star-forming regions at different ages, it is possible to obtain constraints on gas-dissipation timescales. Furthermore, the study of accretion also gives us insight into the connection between the central star and its circumstellar disk, presumably through a magnetic field.

Here we report on a comprehensive study of disk accretion and related phenomena in four nearby associations of young stars: η Chamaeleontis (η Cha; ∼6 Myr), β Pictoris (β Pic; ∼12 Myr), TW Hydrae (TWA; ∼8 Myr), and Tucanae-Horologium (Tuc-Hor; ∼30 Myr). Many of these stars have been identified based on their X-ray emission and later confirmed as young by the detection of lithium in optical spectra. Their membership in the associations is supported by several lines of evidence, including measurements of radial velocities, proper motions, and distances (when possible). For a recent review of the properties of these groups, see Zuckerman & Song (2004). By investigating accretion in those four associations spanning an age range from 6 to 30 Myr and combining the results with literature data for younger regions (e.g., Mohanty et al. 2005), we are able to determine the fraction of accretors as a function of age. The high-resolution, high signal-to-noise ratio (S/N), multiepoch spectra that we have collected allow us to distinguish accretors from nonaccretors reliably, using line shapes of Hα and other diagnostics. Since chromospheric activity influences the same emission lines as accretion, ambiguity is unavoidable for a few objects, although in most cases this problem can be mitigated by combining information from different lines and analyzing line profiles. We can also identify spectroscopic binaries whose complex line profiles may mimic accretion. In addition, by deriving projected rotational velocities ($v \sin i$) for our targets, we will explore for the first time whether there is any evidence for "disk locking" (i.e., for accretors being preferentially slow rotators) at these older ages. We are also able to investigate time variability of emission lines in a number of objects.

2. OBSERVATIONS AND SPECTRAL ANALYSIS

We have obtained a total of ∼650 high-resolution spectra of 100 likely members of four nearby associations (η Cha, TWA, β Pic, and Tuc-Hor) with the echelle spectrograph MIKE at the

TABLE 1
OBSERVATION RECORD

Date (UT)	Targets (In Parentheses: the Number of Observations if >1)
2004 Dec 04	η Cha 1, η Cha 11, η Cha 7, TWA 19A, TWA 5A, TWA 9A, AU Mic (3), AO Men (2), β Pic, GJ 3305 (2), HIP 23309 (2).
2004 Dec 05	η Cha 4, η Cha 5, η Cha 7, η Cha 10, η Cha 11, η Cha 12, AO Men (2), GJ 3305 (2), HIP 23309 (2), TW Hya (2), TWA 5A, TWA 9A, TWA 19A.
2004 Dec 06	η Cha 3, η Cha 4, η Cha 6, η Cha 7, η Cha 9, η Cha 11, η Cha 13, TW Hya (2), TWA 5A, TWA 6, TWA 7, TWA 8A, TWA 9A, TWA 19A, AO Men (2), AU Mic (5), β Pic (2), GJ 3305 (2), HIP 23309 (2).
2005 Jan 29.....	η Cha 1 (2), η Cha 10 (2), η Cha 11, η Cha 12 (2), η Cha 13, η Cha 3, η Cha 4 (2), η Cha 5, η Cha 6 (2), η Cha 9 (2), TW Hya, TWA 2A, TWA 3A, TWA 3B, TWA 4A, TWA 6, V343 Nor.
2005 Jan 30.....	η Cha1, η Cha 3 (2), η Cha4, η Cha 5 (2), η Cha6, η Cha10, η Cha12, η Cha13 (2), TWA 2A, TWA 3A, TWA 3B, TWA 4A, TWA 5A, TWA 6, TWA 7, TWA 8A, TWA 9A, TWA 9B, TWA 11A, TWA 11B, TWA 13A, TWA 13B, TWA 19A, TWA 19B, AO Men, β Pic (2), HD 35850, HIP 23309, V343 Nor, CD−53544, CD−60416, CPD−64120, GSC 8056−0482, GSC 8491−1194, GSC 8497−0995, HD 13183, HD 13246, HD 8558, HD 9054, HIP 16853, HIP 21632, HIP 22295, HIP 30030, HIP 30034, HIP 32235, HIP 33737, HIP 9141, TYC 5882−1169, TYC 7600−0516.
2005 Jan 31.....	η Cha 1, η Cha 4, η Cha 11 (2), η Cha 12, TWA 2A, TWA 4A, TWA 5A, TWA 6, TWA 7, TWA 9A, TWA 10, TWA 12, TWA 13A, TWA 13B, TWA 14, TWA 16, TWA 17, TWA 18, TWA 19A, TWA 19B, β Pic, AO Men, HD 35850, HIP 23309, CD −53 544, CD −60 416, CPD −64 120, GSC 8056−0482, GSC 8491−1194, GSC 8497−0995, HD 13183, HD 13246, HD 8558, HD 9054, HIP 16853, HIP 21632, HIP 30030, HIP 32235, HIP 33737, HIP 9141, TYC 5882−1169, TYC 7600-0516.
2005 Feb 01.....	η Cha 1, η Cha 3, η Cha 4, η Cha 5, η Cha 6 (2), η Cha 9, η Cha 10, η Cha 12 (2), η Cha 13, TW Hya (2), TWA 2A, TWA 4A, TWA 5A, TWA 6, TWA 7, TWA 8A, TWA 8B, TWA 9A, TWA 9B, TWA 10, TWA 12, TWA 13A, TWA 13B, TWA 14, TWA 17, TWA 18, TWA 19A, TWA 19B, β Pic, GJ 3305, HD 35850, HIP 23309, V343 Nor, CD −53 544, CD −60 416, CPD −64 120, GSC 8056−0482, GSC 8491−1194, GSC 8497−0995, HD 13183, HD 13246, HD 8558, HD 9054, HIP 16853, HIP 21632, HIP 22295, HIP 30030, HIP 30034, HIP 32235, HIP 33737, HIP 9141, TYC 5882−1169, TYC 7600−0516.
2005 Mar 26	TWA 3A, TWA 3B, HIP 23418.
2005 Mar 27	η Cha 1, η Cha 3, η Cha 4, η Cha 13, TW Hya (2), TWA 2A (2), TWA 5A (4), TWA 6 (2), TWA 7 (2), TWA 8A (2), TWA 8B (2), TWA 15A, TWA 15B, TWA 16, TWA 20, TWA 21, TWA 22, TWA 23, TWA 24, TWA 25, β Pic (2), AO Men, AU Mic (4), BD −17 6128, CD −64 1208, GJ 3305, GJ 799A, GJ 799B, HD 164249, HD 181327, HD 199143, HD 35850 (2), HIP 23309, HIP 23418, HR 7329B, PZ Tel, HIP 105388, HIP 105404, HIP 107345, HIP 107947, HIP 108422, HIP 16853 (2), HIP 21632, HIP 22295, HIP 30030, HIP 30034, HIP 32235, HIP 33737, TYC 5882−1169, TYC 7065−0879 (2), TYC 7600−0516.
2005 Mar 28	η Cha 5, η Cha 6, η Cha 9, η Cha 10, η Cha 11, η Cha 12, TWA 5A (5), TWA 9A (2), TWA 9B (2), TWA 10 (2), TWA 11A (2), TWA 11B (2), TWA 12 (2), TWA 13A (2), TWA 13B (2), TWA 14 (2), TWA 16 (2), TWA 17 (2), TWA 18 (2), TWA 19A (2), TWA 19B (2), TWA 20, TWA 21 (2), TWA 22 (2), TWA 23, TWA 24 (2), TWA 25, AU Mic (3), BD −17 6128 (2), β Pic, CD −64 1208, GJ 799A, GJ 799B, HD 164249, HD 181327, HD 199143, PZTel, V343 Nor, HIP 105388, HIP 105404, HIP 107345, HIP 107947, HIP 108422, HIP 21632, HIP 22295, HIP 30030, HIP 30034, HIP 32235, HIP 33737, TYC 5882−1169, TYC 7600−0516.
2005 Mar 29	TW Hya, TWA 2A, TWA 3A, TWA 4A, TWA 5A (4), TWA 6, TWA 7, TWA 8A, TWA 8B, TWA 9A, TWA 9B, TWA 10, TWA 11A, TWA 11B, TWA 12, TWA 13A, TWA 13B, TWA 14, TWA 15A (2), TWA 15B (2), TWA 17, TWA 18, TWA 19A, TWA 19B, TWA 20 (2), TWA 21 (2), TWA 22 (2), TWA 23 (2), TWA 24, TWA 25 (2), AU Mic (7), BD −17 6128, β Pic (2), CD −64 1208, GJ 799A, GJ 799B, HD 164249, HD 181327, HD 199143, HIP 23418, PZ Tel, HIP 105388, HIP 105404, HIP 107345, HIP 107947, HIP 108422.
2005 Mar 30	TW Hya, TWA 2A, TWA 3A, TWA 3B, TWA 4A, TWA 5A (4), TWA 6, TWA 7, TWA 8A, TWA 8B, TWA 9A, TWA 9B, TWA 10, TWA 11A (13), TWA 11B, TWA 12, TWA 13A, TWA 13B, TWA 14, TWA 15A (2), TWA 15B (2), TWA 16, TWA 18, TWA 19A, TWA 19B, TWA 20 (2), TWA 21, TWA 22, TWA 23 (2), TWA 24, TWA 25 (2), AU Mic (2), BD −17 6128, CD −64 1208, GJ 799A, GJ 799B, HD 164249, HD 181327, HD 199143, HIP 23418, PZ Tel, HIP 105388, HIP 105404, HIP 107345, HIP 107947, HIP 108422.
2005 Jul 19	TWA 2A, TWA 3A, TWA 3B, TWA 4A, TWA 5A, TWA 6, TWA 7, TWA 8A, TWA 8B, TWA 9A, TWA 9B, TWA 12, TWA 13A, TWA 13B, TWA 14, TWA 16, TWA 17, TWA 18, TWA 19A, TWA 19B, TWA 21, TWA 22, TW Hya, AU Mic (2), BD −17 6128 (2), β Pic (5), CD −64 1208 (2), GJ 799A (2), GJ 799B (2), HD 1555A (2), HD 164249 (2), HD 181327 (2), HD 199143 (2), HD 35850, HIP 112312 (2), HIP 112312B (2), HIP 12545 (2), HIP 23418, PZ Tel (2), V343 Nor, CD −53544, CD −60416 (2), CPD −64120 (2), GSC 8056−0482, GSC 8491−1194, GSC 8497−0995, HD 13183 (2), HD 13246 (2), HD 8558 (2), HD 9054 (2), HIP 105388 (2), HIP 105404 (2), HIP 107345 (2), HIP 107947 (2), HIP 108422 (2), HIP 1113 (2), HIP 116748B (2), HIP 116748A (2), HIP 1481 (2), HIP 16853, HIP 1910 (2), HIP 1993 (2), HIP 21632, HIP 22295, HIP 2729 (2), HIP 3556 (2), HIP 490 (2), HIP 9141 (2), TYC 5882−1169, TYC 7600−0516.

Magellan Clay 6.5 m telescope in Las Campanas, Chile. The data were collected during four observing runs between 2004 December and 2005 July. The summary observing log is given in Table 1.

MIKE is a double echelle slit spectrograph, consisting of blue and red arms. For this accretion study, we concentrated on the red spectra, with coverage from 4900 to 9300 Å. With no binning and using the 0.″35 slit, our spectra have a resolution of $R \sim 60{,}000$. The pixel scale was 0.″14 pixel^{-1} in the spatial direction, and about 24 mÅ pixel^{-1} at 6500 Å in the spectral direction. One peculiarity of MIKE is that it produces slanted echelle spectra, that is, the spatial direction of the projected slit is not aligned with the CCD columns. Moreover, this tilt is wavelength dependent. We therefore developed a customized software package in ESO-MIDAS to take the slant into account. The details of the reduction software and procedures used will be described in a forthcoming paper.

Integration times were chosen so that the S/N $\gtrsim$80 per spectral resolution element at 6500 Å, except for the brightest stars, where this would have implied an exposure shorter than 120 s. In those cases, we used the longest exposure time shorter than 120 s that did not saturate the detector, giving S/N ~80–500, depending on seeing.

In this first of a series of papers, we focus on accretion-related emission lines in these spectra. In particular, we have measured

TABLE 2
SUMMARY OF RESULTS: η CHA

Object	Other Name	No. of Spectra	Spectral Type	EW (Å)	EW σ[a] (Å)	10% Width (km s^{-1})	10% Width σ[a] (km s^{-1})	$v \sin i$[b] (km s^{-1})	Comments
η Cha 1	RECX 1	7	K4[c]	−1.2	0.3	103	13	20.9	
η Cha 3	RECX 3	6	M3.25[d]	−2.0	0.2	116	8	10.5	
η Cha 4	RECX 4	8	K7[c]	−3.4	0.6	147	13	6.0	
η Cha 5	RECX 5	6	M4[d]	−8.6	4.3	194	66	8.8	
η Cha 6	RECX 6	7	M2[c]	−5.0	0.4	145	27	20.9	
η Cha 7	RECX 7	3	K6[d]	−1.0	0.3	291	70	29.1	Spectroscopic binary
η Cha 9	RECX 9	6	M4.5[d]	−11.7	2.7	389	54	20.8	He I (6678 Å)
η Cha 10	RECX 10	6	K7[c]	−1.2	0.3	103	13	<5.0	
η Cha 11	RECX 11	7	K4[c]	−3.9	2.1	345	86	16.4	
η Cha 12	RECX 12	8	M2[c]	−5.7	0.5	154	7	15.1	
η Cha 13	ECHA J0843.3−7905	6	M2[c]	−110.8	13.7	435	26	14.5	He I (6678 Å)

[a] Values for σ are the scatter in our multiepoch spectra, not the measurement uncertainty. Errors in EW are 0.2 Å, in 10% width 5 km s^{-1}.
[b] The values for spectroscopic binaries (see last column) might be affected by line blending.
[c] Zuckerman & Song (2004).
[d] Luhman & Steeghs (2004).

the equivalent width (EW) and the full width at 10% of the peak (see § 3) for the Hα emission line. Hα is perhaps the most widely used accretion diagnostic, mainly because it is highly sensitive and detectable even in weak accretors. However, the Hα feature is also affected by chromospheric flares and stellar winds, leading to complex and sometimes ambiguous behavior. For the line-width measurements, the continuum level was determined by a linear fit to the continuum on both sides of the Hα line. By measuring the EW in several continuum regions without strong features, we estimate that the uncertainty of our EW values is on average 0.2 Å. For the 10% widths, the errors are $\sim$5 km s^{-1}. We also looked for other diagnostics, such as He I (5876 and 6678 Å), O I (7773 and 8446 Å), and the Ca II triplet (8498, 8542, and 8662 Å). We measured the projected rotational velocity ($v \sin i$) of each of our targets by χ^2 fitting with a "spun-up" template of a slowly rotating standard. More details on the $v \sin i$ measurements will be provided in a forthcoming paper.

3. ACCRETION SIGNATURES

The strength of the Hα line has long been used to distinguish classical T Tauri stars or accretors (EW $>$ 10 Å) from weak-line T Tauri stars or nonaccretors (EW $<$ 10 Å). It is believed, particularly in the context of the magnetospheric accretion scenario, that in accretors, Hα is produced in the gas falling in from the disk inner edge onto the star. In nonaccretors, Hα emission originates only from chromospheric activity, and thus is generally weaker. Furthermore, the Hα profiles of accretors tend to be much broader, due to the high velocity of the accreting gas as well as Stark broadening, and asymmetric, as a result of inclination effects and/or absorption by a wind component.

Since the measured EW of Hα, and thus the threshold for classifying an object as an "accretor," depends on the spectral type, White & Basri (2003) proposed the full width of the line at 10% of the peak (hereafter, 10% width) as a more robust diagnostic. Based on the presence or absence of veiling in their stellar spectra, they proposed that 10% width >270 km s^{-1} indicates accretion. Using physical reasoning as well as empirical findings, Jayawardhana et al. (2003) adopted 200 km s^{-1} as a more reasonable accretion cutoff for the very low mass regime (i.e., brown dwarfs), but cautioned that it should be used in combination with additional diagnostics whenever possible. Intriguingly, Natta et al. (2004) have shown that the Hα 10% width correlates very well with the mass accretion rate derived by other means. Thus, the 10% width not only appears to be a good qualitative indicator of accretion but also gives a quantitative estimate of the infall rate. Here we use both the EW and the 10% width as diagnostics, because accretion should affect both values. On the other hand, if the line profile is broadened due to binarity or fast rotation, we expect high 10% width, but the EW should be comparable to those of nonaccretors. We also investigate the presence or absence of certain other emission lines, in particular O I (8446 Å), He I (6678 Å), and Ca II (8662 Å), that are often associated with accretion as well (see discussion and references in Mohanty et al. 2005). In particular, the He I (6678 Å) emission feature appears to be a good indicator of ongoing accretion. As shown by Gizis et al. (2002), chromospherically active stars often show this line in emission, but at a very weak level with EW below 0.25 Å. For our spectra, this is in the range of our detection limit and thus not significant. In a few cases, this line has been reported to be in emission during chromospheric flare events (Montes et al. 1998; Martin & Ardila 2001) with EW of a few Å; thus, attributing nonpersistent emission in this line to accretion might be problematic. However, if we clearly detect He I (6678 Å) in emission in all spectra for a given star, the object is very likely accreting.

We have measured the Hα EW and 10% width in all the spectra in hand for all late-type stars in our sample (see § 2). For objects where we see Hα in emission, the average values and their standard deviations are reported in Tables 2–5; the $\sigma_{\rm EW}$ gives an indication of the line's variability. We note that these values are in many cases clearly higher than our measurement uncertainties (see § 2), demonstrating that many stars in our sample show emission-line variability (see § 6). The tables also indicate the presence of the He I (6678 Å) emission feature, which is an additional diagnostic for ongoing accretion. In the four panels of Figure 1, we plot the Hα EW versus 10% width for members of each of the four stellar associations. This plot is a good way to identify likely accretors in each group, using the criteria discussed above. We show Hα profiles for selected objects in Figures 2 and 3.

Among η Cha cluster members, one star, ECHA J0843.3−7905 or η Cha 13, shows strong signs of accretion, with large Hα equivalent and 10% widths, comparable to those seen in classical T Tauri stars, and a host of other broad emission lines. η Cha 9 also makes the cut as an accretor, based on both its EW and 10% width, as well as the presence of He I (6678 Å). Two other members, η Cha 7 and 11, exhibit broad-line wings, with 10% widths

TABLE 3

SUMMARY OF RESULTS: TW HYDRAE

Object	Other Name	No. of Spectra	Spectral Type	EW (Å)	EW σ[a] (Å)	10% Width (km s^{-1})	10% Width σ[a] (km s^{-1})	$v \sin i$[b] (km s^{-1})	Comments
TW Hya	TWA 1	12	K7[c]	−172.5	44.7	425	35	10.6	He I (6678 Å)
TWA 2A	CD−29 8887A	9	M2e[d]	−1.8	0.2	134	17	12.8	
TWA 3A	Hen 3−600A	5	M3e[d]	−22.6	2.9	262	4	11.6	Spectroscopic binary, He I (6678 Å)[e]
TWA 3B	Hen 3−600B	4	M3.5[d]	−6.1	0.9	153	13	12.2	
TWA 5A	CD−33 7795A	24	M1.5[d]	−11.5	4.9	360	54	59.0	He I (6678 Å)
TWA 6	TYC 7183−1477	10	K7[c]	−3.4	0.4	409	42	79.5	Spectroscopic binary
TWA 7	TYC 7190−2111	9	M1[c]	−5.8	0.9	109	8	<5.0	
TWA 8A	...	8	M2[d]	−8.0	1.4	133	29	<5.0	
TWA 8B	...	6	...	−13.3	1.8	119	10	11.2	
TWA 9A	CD−36 7429A	11	K5[d]	−2.1	0.5	135	21	11.3	
TWA 9B	CD−36 7429B	7	M1[d]	−4.3	0.6	108	12	8.4	
TWA 10	GSC 07766−00743	6	M2.5[c]	−13.6	9.6	199	97	6.3	He I (6678 Å)
TWA 11B	HR 4796B	5	M2.5[d]	−3.5	0.6	116	10	12.1	
TWA 12	RX J1121.1−3845	7	M2[d]	−4.8	0.9	136	28	16.2	
TWA 13A	RX J1121.3−3447N	8	M1e[d]	−3.0	0.7	129	24	10.5	
TWA 13B	RX J1121.3−3447N	8	M2e[d]	−3.0	0.7	134	26	10.3	
TWA 14	...	7	M0[d]	−10.7	7.8	291	61	43.1	Spectroscopic binary
TWA 15A	...	5	M1.15[d]	−8.8	0.5	156	2	21.3	
TWA 15B	...	5	M2[d]	−8.6	1.4	193	16	32.3	
TWA 16	...	6	M1.5[d]	−4.0	0.8	119	12	7.9	
TWA 17	...	6	K5[d]	−3.2	0.4	290	25	49.7	Spectroscopic binary
TWA 18	...	7	M0.5[d]	−3.3	0.4	179	11	24.1	
TWA 19B	HD 102458B	8	K7[d]	−2.2	0.4	239	45	48.7	Spectroscopic binary
TWA 20	A2 146	6	M2[d]	−3.1	0.2	273	28	[f]	Spectroscopic binary
TWA 22	SSS 1017−5354	7	M5[c]	−11.5	2.0	111	10	9.7	
TWA 23	SSS 1207−3247	6	M1[c]	−2.4	0.2	126	3	14.8	
TWA 24	GSC 8644−0802	5	K3[c]	−0.3	0.2	137	29	13.0	
TWA 25	TYC 7760−0283	6	M0[c]	−2.4	0.5	128	10	11.8	

[a] Values for σ are the scatter in our multiepoch spectra, not the measurement uncertainty. Errors in EW are 0.2 Å, in 10% width 5 km s^{-1}.
[b] The values for spectroscopic binaries (see last column) might be affected by line blending.
[c] Zuckerman & Song (2004).
[d] de la Reza & Pinzon (2004).
[e] For all measurements, only spectra were used where we see no doubled lines. Line widths should, therefore, not be affected by binarity.
[f] TWA 20 is a spectroscopic binary; it was not possible to obtain a $v \sin i$ fit with acceptable reliability.

TABLE 4

SUMMARY OF RESULTS: β PIC MOVING GROUP

Object	Other Name	No. of Spectra	Spectral Type	EW (Å)	EW σ[a] (Å)	10% Width (km s^{-1})	10% Width σ[a] (km s^{-1})	$v \sin i$[b] (km s^{-1}	Comments
AO Men	HIP 29964	9	K6/7[c]	−0.6	0.1	122	15	16.0	
Au Mic	HIP 102409	26	...	−2.3	0.8	134	52	8.5	
BD −17 6128	HD 358623	7	K7/M0[d]	−0.5	0.2	118	13	14.6	
CD −64 1208	CPD −64 3950	6	K7[c]	−2.9	0.5	494	23	102.7	Spectroscopic binary
GJ 3305	...	8	M0.5[c]	−2.2	0.3	128	15	5.3	
GJ 799A	...	6	M4.5e[c]	−10.5	1.4	96	3	10.6	
GJ 799B	...	6	M4.5e[c]	−8.9	0.8	138	13	17.0	
HIP 12545	BD +05 378	2	M0[c]	−0.6	0.0	95	5	9.3	
HIP 23309	CD −57 1054	10	M0.5[c]	−0.8	0.2	108	13	5.8	
HIP 23418A	GJ 3322A	...	M3[c]	−6.6	...	108	...	7.7	
HIP 23418B	GJ 3322B	...	...	−6.1	...	116.6	...	21.0	
HIP 112312A	V* WW PsA	2	M4e[c]	−6.6	0.1	105	4	14.0	
HIP 112312B	...	2	M4.5e[c]	−8.2	0.5	137	4	24.3	

[a] Values for σ are the scatter in our multiepoch spectra, not the measurement uncertainty. Errors in EW are 0.2 Å, in 10% width 5 km s^{-1}.
[b] The values for spectroscopic binaries (see last column) might be affected by line blending.
[c] Zuckerman & Song (2004).
[d] de la Reza & Pinzon (2004).

TABLE 5
SUMMARY OF RESULTS: TUC-HOR

Object	Other Name	No. of Spectra	Spectral Type	EW (Å)	EW σ[a] (Å)	10% Width (km s^{-1})	10% Width σ[a] (km s^{-1})	$v \sin i$ (km s^{-1})	Comments
CD −53 544	TYC 8491− 656−1	4	K6 Ve[b]	−1.4	0.2	403	48	82.2	Fast rotator
CD −60 416	TYC 8489− 1155−1	5	K3/4[b]	−0.5	0.0	110	19	10.1	
CPD −64 120	TYC 8852− 264−1	5	K1Ve[b]	−0.2	0.1	103	15	30.2	
GSC 8056−0482	...	4	M3Ve[b]	−5.3	0.4	177	26	34.2	
GSC 8491−1194	...	4	M3Ve[b]	−4.1	0.4	99	1	12.8	
GSC 8497−0995	...	4	K6Ve[b]	−0.6	0.2	96	12	6.6	
HIP 1910	BPM 1699	2	M1[b]	−1.6	0.1	132	2	19.0	
HIP 1993	GSC 08841−00145	2	M1[b]	−1.0	0.1	97	8	7.1	
HIP 2729	HD 3221	2	K5V[b]	−0.7	0.3	467	28	127.5	Fast rotator
HIP 3556	GJ 3054	2	M3[b]	−0.8	0.0	107	12	<5.0	
HIP 107345	BPM 14269	6	M1[b]	−1.4	0.2	114	13	<5.0	

[a] Values for σ are the scatter in our multiepoch spectra, not the measurement uncertainty. Errors in EW are 0.2 Å, in 10% width 5 km s^{-1}.
[b] Zuckerman & Song (2004).

above 300 km s^{-1}, but their emission is relatively weak (Fig. 2). Lyo et al. (2004) found η Cha 7 to be a double-line spectroscopic binary. Our Hα profiles of it could well result from the blending of two emission lines from the two binary components (Fig. 2). Besides, it does not show any other accretion-related emission. Thus, we conclude that η Cha 7 is not an accretor. The Hα profile of η Cha 11 also appears to consist of more than one component (see Fig. 2 and § 6), but this target does not show any other signs of binarity (Zuckerman & Song 2004). Whether it is a binary or not, the broad red absorption feature in its Hα profile, seen at several epochs, is hard to explain without invoking high-velocity infalling material; therefore, we classify η Cha 11 as an accretor. The star η Cha 5 is at the boundary between accretors and nonaccretors. Of our five spectra of η Cha 5, only one shows broad Hα (Fig. 2). The average 10% width is ~200 km s^{-1}, well below the White & Basri (2003) threshold. Furthermore, none of its spectra shows other definitive signs of accretion such as He I (6678 Å) emission. Given these findings, we conclude that it was not accreting during our observations. On the other hand, Lawson et al. (2004) detected broad Hα emission with more than 300 km s^{-1} 10% width in a single spectrum, and concluded that η Cha 5 is accreting at a significant level. Thus, the status of this object is questionable; it appears to show some sporadic accretion, indicating that accretion variability can be quite substantial on long timescales. Since it is nonaccreting in our multiepoch spectra, we do not count it as an accretor in the remainder of this paper.

Both ground-based and *Spitzer* mid-infrared data are available for members of the η Cha group. The L'-band (3.8 μm) survey by Haisch et al. (2005) found infrared excess for only two stars, η Cha 11 and 13, both of which we classify as accretors above. The *Spitzer* IRAC photometry by Megeath et al. (2005) indicates 4–10 μm excess emission for four stars in our sample, η Cha 5, 9, 11, and 13 (called 15 in their paper), where η Cha 5 and 9 show excess only at wavelengths >4 μm. The IRAC color excess for η Cha 5 confirms that it still might be able to accrete sporadically, as seen by Lawson et al. (2004), but not in our spectra. It is intriguing that there is no L'-band, but IRAC color excess plus evidence for at least sporadic accretion in η Cha 5 and 9. This could imply substantial grain growth and/or partial clearing of the inner disk while they are still accreting. Thus, these objects might have inner disks depleted of dust, but with substantial amounts of gas. This may also be the case with the accreting star TW Hydrae (see below).

In the TW Hydrae association, two members, TW Hya and Hen 3-600A (TWA 3A), stand out as accretors based on their Hα emission, as well as the presence of other emission lines such as He I (6678 Å). Both had been identified before, although not in a systematic survey (Muzerolle et al. 2000; Mohanty et al. 2003). Based on mid-infrared photometry of TWA members known at the time, Jayawardhana et al. (1999b) reported excesses consistent with inner disks for these two accretors (as well as the HD 98800 quadruple system and the A star HR 4796A; also see Jayawardhana et al. 1998). Recent *Spitzer* photometry indicates that for both stars, the spectral energy distribution (SED) does not turn over even by 160 μm, again consistent with their status as stars with active accretion disks (Low et al. 2005). While TW Hya is accreting, shows significant mid-infrared excess, and has a face-on disk resolved in scattered light (e.g., Krist et al. 2000) and in the millimeter (Wilner et al. 2003), it appears to lack near-infrared excess. Based on model fits to the SED and the millimeter image, there is evidence for partial clearing of the innermost few AU of its disk (Calvet et al. 2002). In the case of the Hen 3−600 binary system with roughly equal mass companions (separation 1.″4 or ~70 AU), it is interesting that only the primary shows signs of accretion, as well as mid-infrared excess (Jayawardhana et al. 1999a).

Two more objects show emission-line characteristics typical for accretors in at least a few spectra: TWA 10 makes the cut as an accretor based on its EW, but the 10% width is at the borderline. A closer examination of the line profiles shows a burstlike event in our time series (see § 6). During this event, it has increased line width in Hα and He I (6678 Å) emission, as well as a strongly asymmetric profile, which is often seen in accreting T Tauri stars. Another interesting case is TWA 5A; this object has broad Hα emission, but again the values are influenced by a burst event in our time series. During this burst, both EW and 10% width clearly exceed the adopted border between accreting and nonaccreting objects. In the remaining spectra, the 10% width is still very high, but the EW is around 10 Å. Again, He I (6678 Å) is detected, but only during the burst event. We examine the Hα variability of TWA 5A in detail in § 6. TWA 5A has previously been suspected to be an accretor, based on its broad and variable Hα emission (Mohanty et al. 2003).

Although both TWA 10 and TWA 5A show emission-line spectra resembling features seen in accreting stars, the recent analysis of their infrared SEDs obtained from *Spitzer* casts doubts on their spectroscopic classification as accretors (Low et al. 2005). For both objects, the fluxes (or upper limits) at 24, 70, and 160 μm are consistent with pure photospheric emission, without any evidence for excess emission due to disks. This clearly separates them from

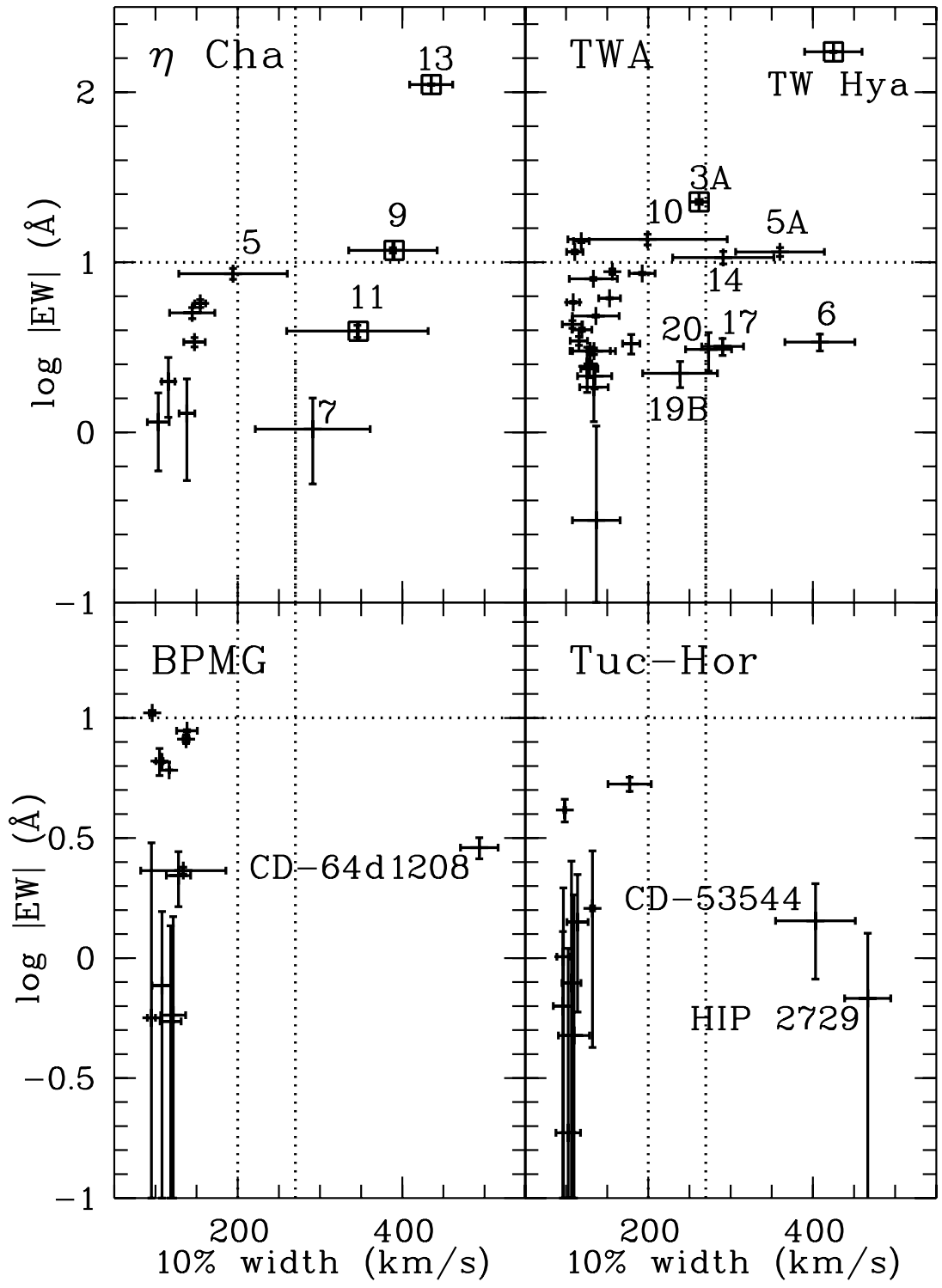

FIG. 1.—Hα 10% width vs. equivalent width for all four groups. The adopted boundaries between accretors and nonaccretors are shown as dotted lines (see discussion in § 3). Specific objects discussed in the text are labeled. Objects classified as accretors in § 3 are marked with squares. The error bars do not correspond to the measurement uncertainty, which is ∼0.2 Å in EW and ∼5 km s^{-1} in 10% width, but to the scatter in our multiepoch data.

the accretors TW Hya and Hen 3−600, whose infrared luminosities are enhanced by several orders of magnitude. Given the nondetection of a disk at mid- and far-infrared wavelengths with the high sensitivity of *Spitzer*, ongoing accretion is unlikely for these two objects. Thus we classify both of them as nonaccretors. The striking, but not persistent, emission-line spectrum is, in both cases, probably due to magnetic activity. As discussed above, chromospheric flares can possibly lead to He I (6678 Å), as well as broad Hα emission. Although it is still doubtful how a flare can also account for the profile variations seen in TWA 10 and TWA 5A, chromospheric activity appears to be the best explanation for the observed behavior. The extremely broad Hα line of TWA 5A is also affected by its fast rotation (see § 5) and binarity. The object is a known roughly equal-mass AO binary (Brandeker et al. 2003), and there are indications for one of the components being a spectroscopic binary itself (Torres et al. 2003). These two

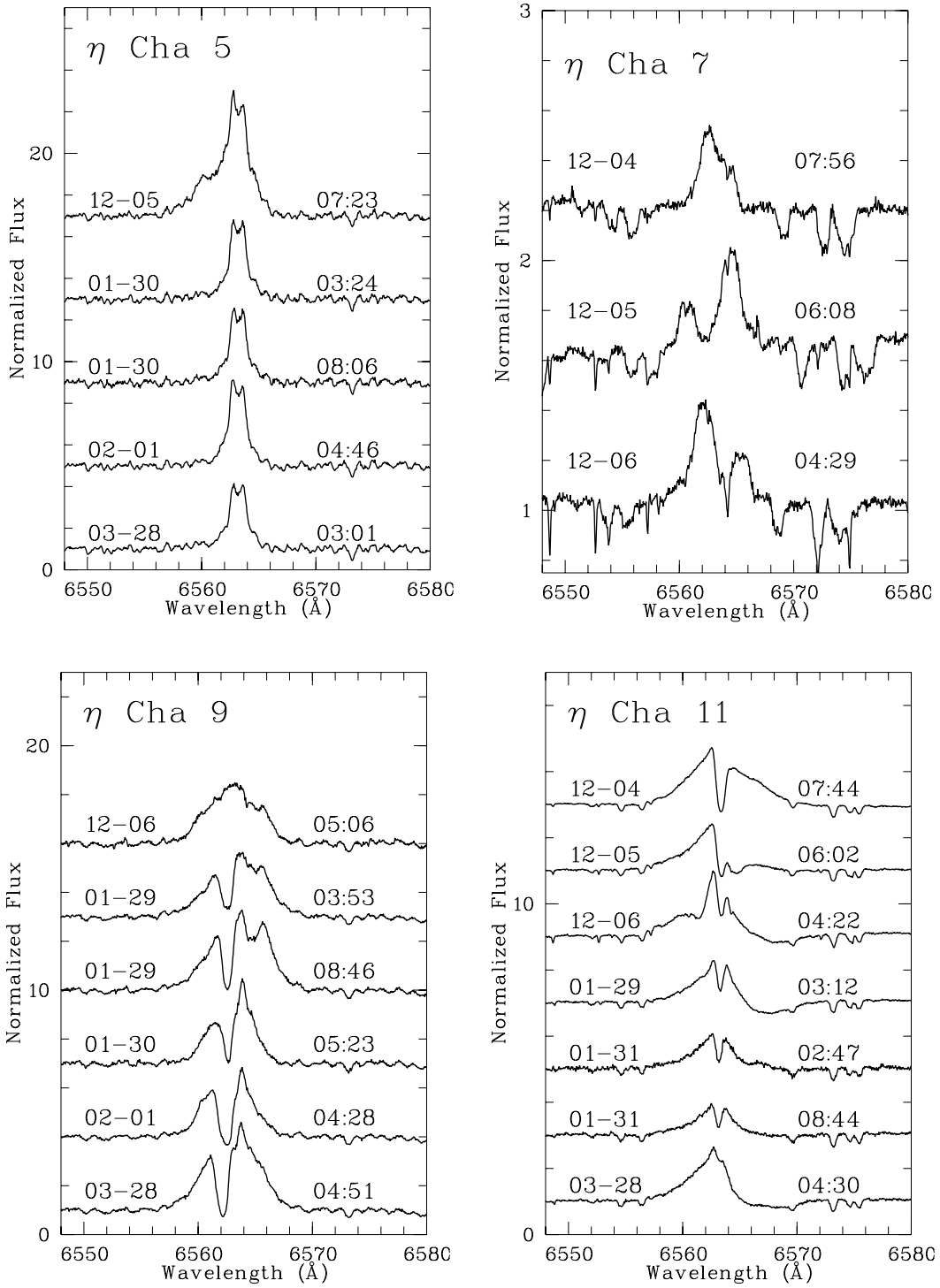

FIG. 2.—Hα time series for selected stars in the η Cha group in chronological order (*from top to bottom*) with UT date and time. Profiles from the different epochs have been shifted by arbitrary units for clarity. All profiles are normalized to the continuum.

cases demonstrate that caution has to be applied when interpreting emission-line spectra of young stars. Multiepoch, multiwavelength data have to be used for a reliable characterization of T Tauri stars.

Five other objects (TWA 6, 14, 17, 19B, and 20) have large 10% widths, but the emission is rather weak. Our multiepoch spectra show evidence of binarity in all five cases (e.g., double-peaked Li I 6708 Å), suggesting that line broadening is the result of the blending of two components rather than high-velocity infalling gas. Perhaps not surprisingly, the same five, along with TWA 5A, have the largest measured $v \sin i$ in the group (see Tables 2–5), probably due to the blending of absorption lines of the two components in the spectra. Furthermore, complementary accretion indicators such as He I emission are absent (or seen in absorption) in the spectra of these five objects. In summary, we conclude that TW Hya and Hen 3−600A are the only accreting stars in our TWA sample. In addition, one of the four young brown dwarfs that are likely members of the TWA, 2MASSW J1207334−393254, is also known to be accreting (Gizis 2002; Mohanty et al. 2003). We have analyzed its variable accretion signatures in two recent papers (Scholz et al. 2005; Scholz & Jayawardhana 2006).

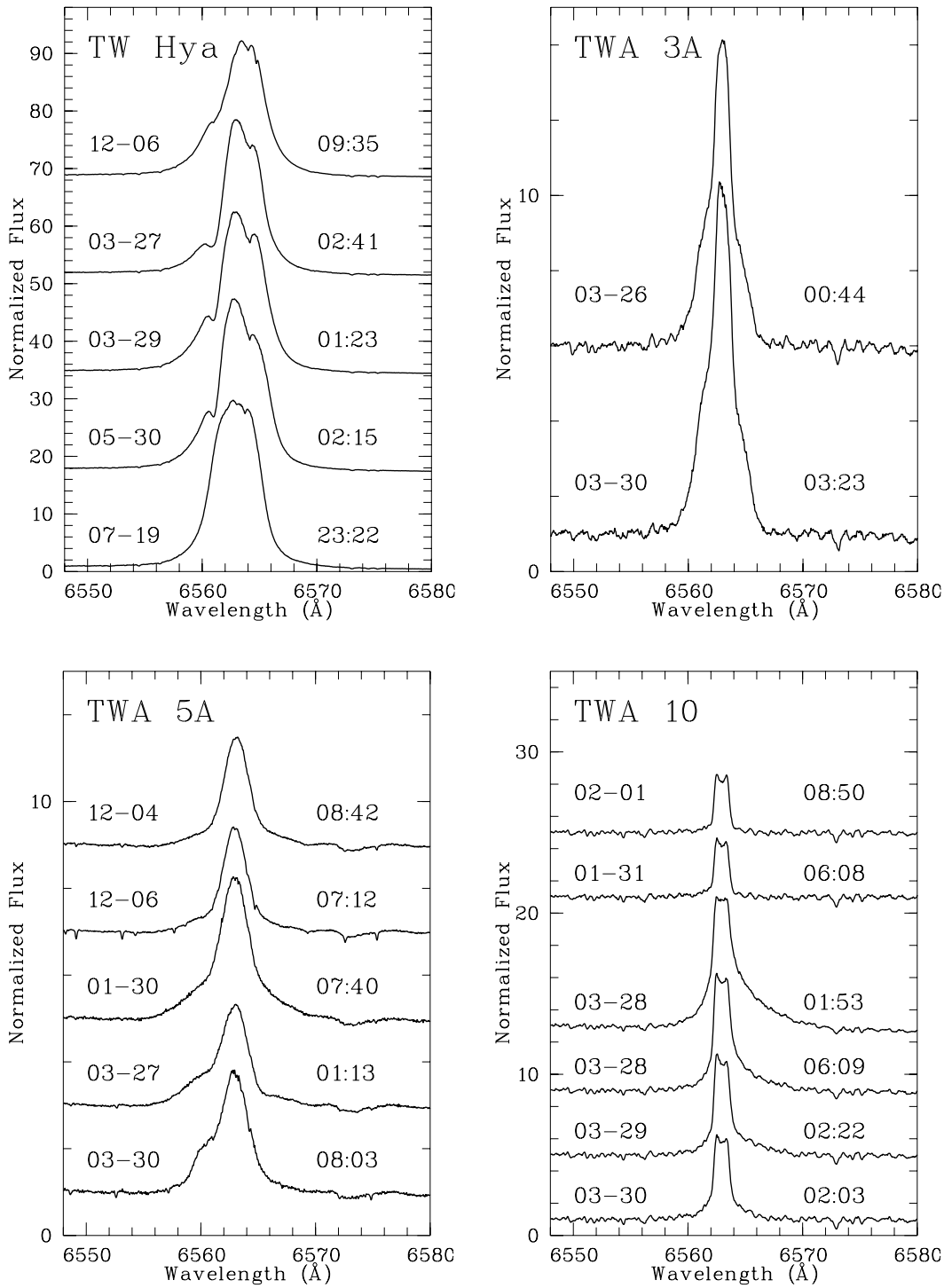

FIG. 3.—Hα time series for selected stars in the TW association in chronological order (*from top to bottom*) with UT date and time. Profiles from the different epochs have been shifted by arbitrary units for clarity. All profiles are normalized to the continuum.

Of the β Pic moving group members in our sample, none shows definitive evidence of ongoing accretion. CD −64 1208 does have a large 10% width, but it is clearly a spectroscopic binary, with line blends accounting for the broad wings; its Li I absorption line is double peaked. The Hα EW is very small, and it does not exhibit any other emission lines associated with accretion. We note that AU Mic, which has a resolved dust disk (Kalas et al. 2004), does not appear to be accreting.

Among Tuc-Hor moving group members in our sample, two (CD −53 544 and HIP 2729) have large Hα 10% widths. We do not find evidence for binarity in either case, but both are fast rotators, with $v \sin i \sim 80$ and $\sim$130 km s^{-1}, respectively. Neither exhibits other accretion-related emission lines. The photospheric lines are clearly broadened by rotation, and the same could account for the broad Hα. Thus, we do not find any accretors in the Tuc-Hor group either. For this group, Mamajek et al. (2004) carried out a mid-infrared survey, but did not find excess emission for any star, indicating that inner circumstellar disks are optically thin and undetectable at the age of Tuc-Hor.

4. FREQUENCY AND LIFETIME OF ACCRETING DISKS

Based on our comprehensive, multiepoch spectroscopic survey, supplemented with previously published results, we find that 3 of the 11 late-type stars in η Cha (27^{+19}_{-14}%) and 2 of the 32 targets in the TWA (6^{+7}_{-4}%) show evidence of ongoing accretion. None of the 21 β Pic and 36 Tuc-Hor targets in our survey appears to be accreting. This corresponds to upper limits on the accretor frequency of 13% for β Pic and 8% for Tuc-Hor (95% confidence). As shown in Figure 4, these accretor fractions are well below those found for younger ($\sim$1–5 Myr) star-forming regions, where the values are generally higher than 30% (Mohanty et al. 2005). Except in the case of η Cha (where we are necessarily limited by the small number of known members), these lower accretion disk frequencies at older ages can no longer be dismissed as being based on very small samples. Furthermore, the fact that we have collected multiepoch spectra for our targets reduces (but does not eliminate) the likelihood that we have missed some nonsteady accretors in this sample.

To probe the evolution of accretion in these young groups, a critical assessment of their ages is important. For η Cha, we adopt the most recent age estimate of 6^{+2}_{-1} Myr, based on a comparison of the observed HR diagram with evolutionary tracks (Luhman & Steeghs 2004). This value is consistent with previous estimates. Webb et al. (1999) discuss different age measurements for the TW Hydrae group, and conclude that the most probable age is $\sim$8 Myr. Recently, Lawson & Crause (2005) found that the TW Hydrae group has two spatially distinct subgroups, whose ages differ by a factor of 2. Based on rotation periods and HR diagrams, they argue that the objects TWA 14–19 are likely older by a factor of 2 than the objects TW Hydrae and TWA 2–13 (TWA 20–25 are not included in their study). From the Li EW, probably the most reliable observational signature to assess the (relative) ages of young stars, there is, however, no evidence for two subgroups with significantly different ages in the TW Hydrae association (Zuckerman & Song 2004). At least the M-type objects TWA 14, 15, and 18 should have depleted their lithium if they were much older than 10 Myr, which is not seen in the data (see Zuckerman & Song 2004, their Fig. 3). In addition, the comparison between the rotation periods of the potential subgroups is clearly hampered by small-number statistics. Thus, we decided to treat TW Hydrae as a uniform group with an age of $\sim$8 Myr.

For the β Pic moving group, both kinematic and evolutionary track diagnostics give an age of $\sim$12 Myr (Zuckerman & Song 2004). For these three groups, the age uncertainty is probably a few Myr. However, using the Li abundance as an age indicator, Zuckerman & Song (2004, their Fig. 3) have convincingly shown that β Pic is clearly older than TW Hydrae, and that TW Hydrae is older than η Cha. Finally, the most probable age for Tuc-Hor is $\sim$30 Myr (Zuckerman & Song 2004; Torres et al. 2000).

By combining these age estimates with our accretor frequencies, we can set strong constraints on the lifetime of accreting disks (see Fig. 4): disk accretion appears to cease or dip below measurable rates by about 10 Myr for most late-type stars. Longer lived accretors must be rare, given that we did not find any among 57 targets in β Pic and Tuc-Hor groups. At $\sim$12 Myr, the estimated age of the β Pic group, the accretor fraction drops below 13% (95% confidence limit); at $\sim$30 Myr, the age of Tuc-Hor, it is $<$8%. These numbers are in full agreement with constraints from previous studies, which find that accretor frequency and accretion rates drop significantly between 4 and 10 Myr (e.g., Muzerolle et al. 2000; Sicilia-Aguilar et al. 2005). This also provides an indirect constraint on the timescale for gas dissipation in the inner disks and, in turn, on the timescale for gas-giant planet formation. Interestingly, the lifetime we derive for gas accretion is roughly consistent with that found for dust in inner disks in previous near- and mid-infrared studies (e.g., Haisch et al. 2001; Jayawardhana et al. 1999b).

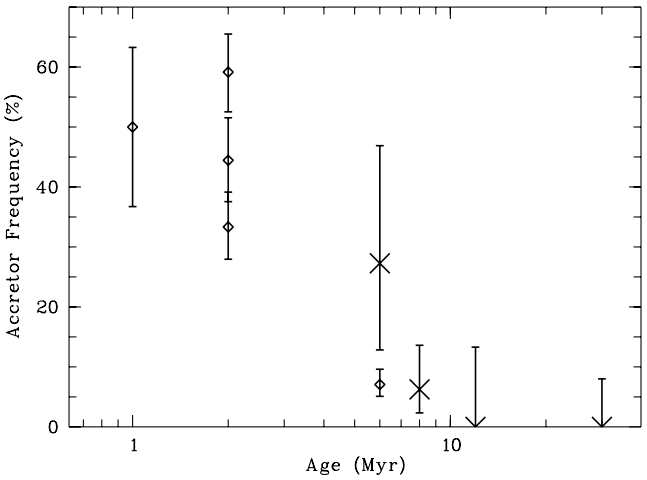

FIG. 4.—Accretor frequency as a function of age. Diamonds mark values from Mohanty et al. (2005) for K0-M4 stars in different star-forming regions, i.e., objects with comparable spectral type but lower ages than our targets. Crosses are the data points for η Cha, TWA, β Pic, and Tuc-Hor from our study. Error bars are 1 σ uncertainties for detections and 95% confidence upper limits for nondetections. Age uncertainties are $\sim$2 Myr except for Tuc-Hor, where the error is more likely 5 Myr. The *relative* ages for our four target groups are more reliable than absolute values. (see § 4).

5. ACCRETION-ROTATION CONNECTION?

Over the years, a number of studies have investigated the connection between the presence of disks and stellar rotation. In the magnetospheric accretion scenario, gas from the inner disk is thought to be channeled by the stellar magnetic field. In that case, one would expect the field lines to connect the star to the disk, which may prevent the star from spinning up (or at least reduce the spin-up), as it contracts during the pre–main-sequence phase. This process is often referred to as "disk locking" (Camenzind 1990; Koenigl 1991; Shu et al. 1994). In other words, we might expect accreting stars to be preferentially slow rotators compared to their peers. Indeed, initial studies by Edwards et al. (1993) found a correlation between rotation period and near-infrared color excess, interpreted as a connection between star and disk. Although this result has been confirmed, e.g., by Herbst et al. (2002), other groups fail to detect such a correlation (e.g., Stassun et al. 1999).

One problem with many studies of the disk-rotation connection is the use of near-infrared excess as the disk diagnostic. Due to a variety of effects, e.g., dust settling and inner-disk clearing, near-infrared photometry is not a very robust disk indicator. Mid-infrared data are much more reliable for this purpose, and are now available for most of our targets (Jayawardhana et al. 1999b; Low et al. 2005; Megeath et al. 2005). Studies with the aim of investigating the connection between mid-infrared emission and rotation are underway (e.g., Rebull et al. 2005). However, both near- and mid-infrared signatures probe the *presence* of a dusty disk, and not the *coupling* between star and disk, which is required in the disk-locking scenario. As shown here and elsewhere (e.g., Jayawardhana et al. 2001), the existence of a disk does not necessarily imply a star-disk connection, especially at slightly older ages. Therefore, evidence of ongoing accretion, which signals a direct link between the inner disk and the central star, is a

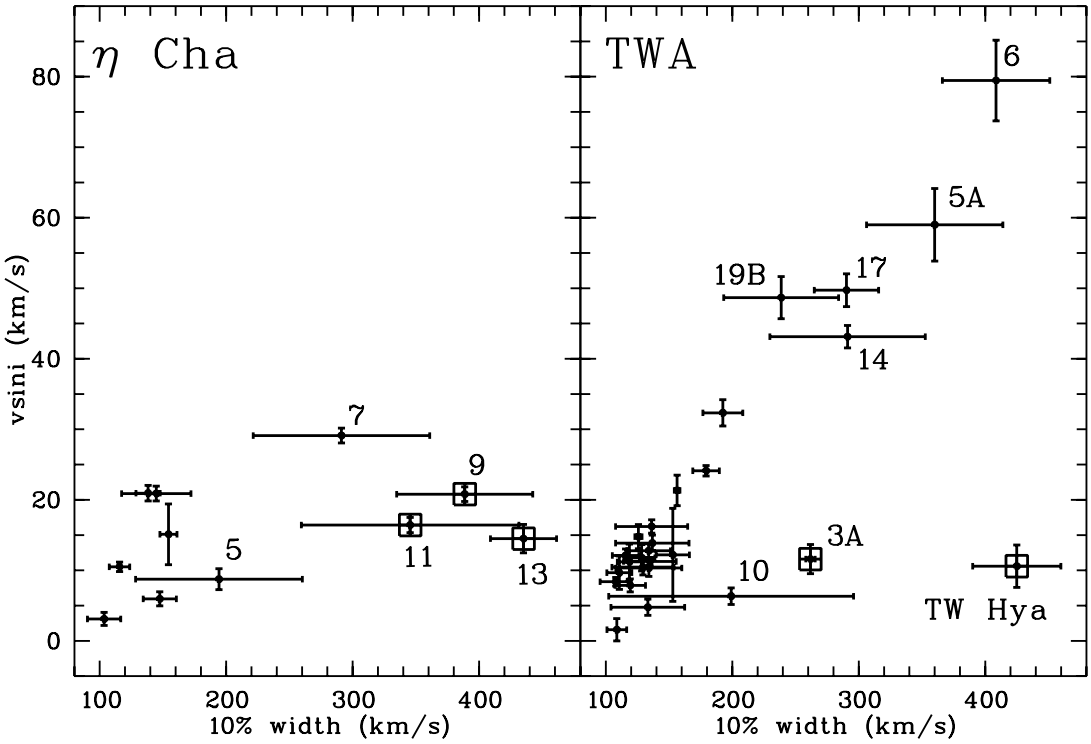

FIG. 5.—Projected rotational velocity $v \sin i$ vs. Hα 10% width for the groups η Cha and TW Hya. Specific objects discussed in the text are labeled. Objects classified as accretors in § 3 are marked with squares. The error bars do not correspond to the measurement uncertainty, but to the scatter in our multiepoch data (see discussion in § 5).

much more sensible diagnostic to correlate with stellar-rotation rates.

To date, there has been, to the best of our knowledge, no study of a possible accretion-rotation connection at ages of ~6–30 Myr. This is a difficult task, because only a few accretors are present at these ages, hampering a reliable statistical comparison of the rotational properties of nonaccretors and accretors. Nevertheless, we decided to probe disk locking at 6–8 Myr using our comprehensive data set for η Cha and TWA. From previous investigations using near-infrared color excess as a disk diagnostic, we expect to see three groups of objects, if disk locking is still at work in our objects (see review by Herbst et al. 2006): (1) slowly rotating stars with a disk, (2) slowly rotating stars without a disk, and (3) rapidly rotating stars without a disk. In some sense, this corresponds to an evolutionary sequence. Stars rotate slowly, as long as they are coupled to their disks. After losing the disk, they still rotate slowly for a certain time, because it takes some time to spin them up. Eventually, they will become fast-rotating objects without disk, after rotational acceleration due to pre–main-sequence contraction. For this simple picture, the critical test is if there are *fast rotators with disks*. Those objects should not exist in a disk-locking scenario, and the most recent investigations of this issue confirm this expectation for 1 Myr old objects, based on near- and mid-infrared photometry (Herbst et al. 2002; Rebull et al. 2005). Here we explore whether the same behavior still holds at 6–8 Myr.

Figure 5 shows the Hα 10% width (an accretion diagnostic) versus the projected rotational velocity ($v \sin i$) for η Cha and TW Hya stars. Since faster rotation would contribute to line broadening, it is not surprising that there appears to be an overall positive correlation between $v \sin i$ and 10% width. In η Cha, there is no obvious difference between accretors and nonaccretors: all stars are relatively slow rotators with $v \sin i \lesssim 20$ km s^{-1} (with one exception, η Cha 9, but here the 10% width is clearly influenced by binarity, see § 6). In the scenario discussed above, we are missing the fast rotators without disk. This may simply indicate that the stars have not had enough time to spin up. In the somewhat older TW Hya group, the two bona fide accretors, TW Hya and Hen 3-600A (TWA 3A), are both slow rotators with $v \sin i < 15$ km s^{-1}. All other nonaccreting objects cover the whole range in rotational velocities, with $v \sin i$ up to 50 km s^{-1} (excluding spectroscopic binaries with blended line profiles). Thus, the available data for the η Cha and TW Hydrae group are consistent with the described disk-locking scenario. Since there are only a few accretors in those two groups, however, small-number statistics are a significant concern.

In η Cha and TWA, rotation periods have been derived for a few objects (Lawson & Crause 2005; Lawson et al. 2001), including some accretors, through photometric monitoring. In both groups, the periods confirm our results from the $v \sin i$ analysis, albeit again based on very few objects. With one exception, all periods measured in η Cha are in the range of 1–20 days, and the two accretors with periods (η Cha 9 and 11) are indistinguishable from the nonaccretors. In TWA, Lawson & Crause (2005) find two rotationally (and spatially) distinct groups of stars (see § 4). We do not see this dichotomy in our $v \sin i$ data, particularly not after excluding the binaries, which have the highest measured $v \sin i$ values (see § 3). In any case, the accretor with a known period (TW Hya itself) belongs to the group of slow rotators with a period of 2.8 days, consistent with our result from the $v \sin i$ versus 10% width plot.

In summary, we find that all accretors in our sample are slow rotators, with $v \sin i \lesssim 20$ km s^{-1}, whereas nonaccretors show a large spread in rotational velocities up to 50 km s^{-1}. This is consistent with a scenario in which rotational braking by coupling between star and disk can operate in low-mass stars for up to ~8 Myr. Given the small numbers of accretors at these ages,

however, this result is of low significance. It clearly needs to be checked with larger samples if/when they become available.

6. EMISSION-LINE VARIABILITY

Many previous studies of young stars have provided evidence of significant variability in the emission lines, particularly Hα, both in intensity and in profile shape (e.g., Johns & Basri 1995; Alencar & Batalha 2002; Scholz et al. 2005). This was one of the reasons to base our accretor-frequency analysis on multiepoch spectra, to avoid significant bias due to variability. In some cases, variability information can be used to obtain a detailed view of the accretion behavior of young stars. Here, we want to use our spectra to assess the Hα variability of our targets.

As indicated by the "error bars" in Figure 1, many of our targets show significant variability in the Hα line in our multiepoch data. Note that these "error bars" do not show the *uncertainty* of our measurements of EW and 10% width, but the *scatter* of the individual measurements of our multiepoch data. In most cases, this scatter, given in Tables 2–5, is much higher than the formal error. Thus, Hα variability is a common phenomenon in the objects in our sample, comparable to the results obtained previously for younger T Tauri stars (e.g., Johns & Basri 1995; Alencar & Batalha 2002).

As can be seen in Figure 1, the objects with evidence of accretion tend to show particularly strong variability. Out of the seven accretors, five show Hα 10% width changes of more than 30 km s^{-1}. Since the 10% width is correlated with accretion rate (Natta et al. 2004), this indicates that the accretion flow in these young stars is often rather unsteady and/or clumpy. Whereas the Hα width is variable in many cases, the shape of the line is more or less constant for most objects. Some objects, however, show distinct profile changes, probably due to accretion, binarity, or chromospheric activity. In Figures 2 and 3, we present the time series of the Hα profiles for some particularly interesting objects, including most of the accretors, which we discuss below.

Two objects, TWA 10 (Fig. 3) and η Cha 5(Fig. 2), show burstlike events in our time series. In both cases, Hα is clearly much stronger and more asymmetric in one spectrum. For TWA 10, we see gradually decreasing Hα intensity after this burst event, with the quiescent level reached after about 2 days. A similar trend is seen in the He I (6678 Å) emission line, which is a good indicator of accretion, but occasionally also appears during flare events (see § 3). In addition, the Hα line appears to be strongly asymmetric during the burst. This hints to a link between the burst and ongoing accretion-rate changes (see § 3), but the lack of mid-infrared emission precludes the existence of a disk for this object (Low et al. 2005). Thus, the spectroscopic behavior is more likely due to a chromospheric flare event. For η Cha 5, we have less information, because the profile change is only apparent in one spectrum. The origin of this event may be a sudden burst of accretion or a chromospheric flare. Lawson et al. (2004) observe a broad Hα profile in their (single) spectrum, indicating that sporadic accretion events may occur in this object.

The Hα time series of η Cha 7(Fig. 2) shows clear signs of binarity (see § 3), even with our sparse time sampling. The profile appears to have two components that move relative to each other. The two objects with the most complex profiles are η Cha 9 and 11. Both objects have been identified as accretors in § 3, and η Cha 9 has a known close companion (Köhler & Petr-Gotzens 2002), whereas there is no indication of binarity for η Cha 11. The Hα line of η Cha 9 (Fig. 2) shows two peaks with a narrow gap in most spectra, where the substructure of the red peak changes on timescales of hours. These changes might be explained by the combined effects of accretion, wind, and binarity. The profile of η Cha 11 (Fig. 2) shows similar structure in some spectra, but it is highly variable in all components. For this object, there is clear evidence of ongoing accretion from the Hα line profile, because we see a highly redshifted, broad absorption feature, i.e., the line has an inverse P Cygni profile, which is often observed in accreting T Tauri stars (Reipurth et al. 1996) and is a clear indication of infalling material. The complexity of the profile probably indicates strong changes in both accretion and wind, as has been found for younger T Tauri stars (e.g., Johns & Basri 1995; Alencar et al. 2005).

The two well-known accretors in TWA, TW Hya and TWA 3A, show very broad and clearly asymmetric profiles (see Fig. 3). Redshifted absorption features, most likely due to infalling material, are visible, as well as blueshifted profile structures, which may be attributed to outflows. The profile changes are, however, not as dramatic as for the objects discussed above.

The Hα variability of TWA 5A was of particular interest to us because it had previously been suspected to be an accretor (Mohanty et al. 2003) and an AO resolved close binary (Brandeker et al. 2003), with roughly equal mass components and a separation of only 54 mas, corresponding to a projected separation of 3 AU at a distance of 55 pc. In addition, previous high-resolution spectra had hinted that one of the AO components might be a spectroscopic binary as well (Torres et al. 2003). Therefore, TWA 5A was monitored in a more extended time series than most of our other targets; in total, we obtained 22 spectra, 17 during the 2005 March observing run.

The intensity of Hα is strongly variable in our time series. The time series of the EW shows a strong burst on the night of March 28, which has a strong influence on the average EW for this object. This burst event coincides with the appearance of He I and Ca II in the spectra (see § 3), which are not or only weakly detected in the remaining spectra. Only during this event, the EW significantly exceeds the adopted threshold between accretors and nonaccretors, whereas the 10% width is always in the regime normally attributed to accretors (see § 3). However, accretion is unlikely to be the origin for the emission, as argued in § 3, because of the nondetection of a disk excess out to the far-infrared. Thus, the profile shape and variability are probably caused by the combined effects of chromospheric activity, rotation, and binarity. Indeed, the spectroscopic signature of the burst shares similarities with previously observed chromospheric flares (Montes et al. 1998; Martin & Ardila 2001). Thus, we attribute this event to a magnetically induced flare.

The general shape of the Hα profile is very similar in all our spectra: it appears to be composed of a broad and a narrow component, where both components clearly change in intensity and relative position (see Fig. 3). We therefore approximated the Hα of TWA 5A with two Gaussians to disentangle the two components. In all spectra, the profile composed of two Gaussians fits the observed profile almost perfectly, as can be seen in Figure 6. The typical σ is 130 km s^{-1} for the broad component and 40 km s^{-1} for the narrow one, corresponding to EW of 10–15 and $\sim$5 Å, respectively.

What is the origin of the broad and narrow components? Perhaps the most likely interpretation is that we observe emission from two strongly magnetically active stars in this binary system. In this case, the very different line widths in the two components might be explained by differences in rotational velocities. If one of the AO-resolved stars is a spectroscopic binary, where both stars are Hα active, this would also allow for a larger line width and thus provide an explanation for the broad component. Another possible explanation for the line profile is that both components arise from one particularly active star in the system, which

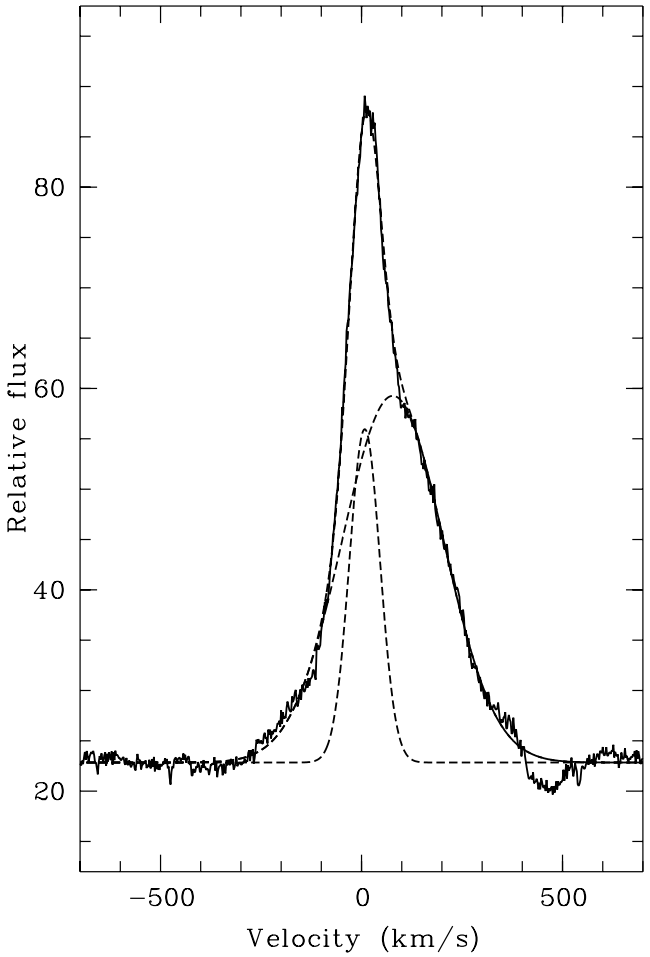

FIG. 6.—Average Hα-line profile for TWA 5A from our time series. The solid line is the observed profile, whereas the dashed lines show results from the decomposition process (narrow component, broad component, and their sum). See discussion in § 6.

exhibits two active regions with different characteristics in the chromosphere.

A more detailed investigation of the complex effects of activity, binarity, and rotation on the Hα feature requires prior knowledge of the properties of the two (or possibly three) stars in the system. Thus, a sophisticated analysis of the photospheric lines in the composite TWA 5A spectrum is necessary to determine rotational velocities for both stars and to investigate the mass and orbital period of a potential third body in the system.

7. CONCLUSIONS

We have carried out an extensive investigation of disk accretion and related phenomena in 100 young stars in four nearby associations that span 6–30 Myr in age. Our study is based on ~650 high-resolution, high S/N multiepoch optical spectra of these targets. We find that disk accretion ceases or dips below measurable levels by ~10 Myr in the vast majority of low-mass stars. This result provides an indirect constraint on the timescale for gas dissipation in inner disks and, thus, gas-giant planet formation. We find that all accretors in our sample are slow rotators, whereas nonaccretors are either slow or fast rotators. This may indicate that stellar rotation is still braked by the disk at 8 Myr, but the small number of accretors at these ages hampers a more detailed investigation of the rotation-accretion connection. Accretors also often exhibit significant time variability in their emission lines, providing evidence for clumpy accretion flows and/or episodic accretion events.

We thank the Las Campanas Observatory staff for their outstanding assistance. This research was supported by Natural Sciences and Engineering Research Council of Canada (NSERC) grants to R. J. and M. H. v. K., as well as University of Toronto startup funds and an SAO subcontract for the Keck Nuller project to R. J. Support was provided to J. C., in part, by an NSERC Undergraduate Student Research Award.

REFERENCES

Alencar, S. H. P., Basri, G., Hartmann, L., & Calvet, N. 2005, A&A, 440, 595
Alencar, S. H. P., & Batalha, C. 2002, ApJ, 571, 378
Brandeker, A., Jayawardhana, R., & Najita, J. 2003, AJ, 126, 2009
Calvet, N., et al. 2002, ApJ, 568, 1008
Camenzind, O. 1990, Rev. Mod. Astron., 3, 234
de la Reza, R., & Pinzon, G. 2004, AJ, 128, 1812
Edwards, S., et al. 1993, AJ, 106, 372
Gizis, J. E. 2002, ApJ, 575, 484
Gizis, J. E., Reid, I. N., & Hawley, S. L. 2002, AJ, 123, 3356
Haisch, K. E., Jr., Jayawardhana, R., & Alves, J. 2005, ApJ, 627, L57
Haisch, K. E., Jr., Lada, E. A., & Lada, C. J. 2001, ApJ, 553, L153
Herbst, W. H., Eislöffel, J., Mundt, R., & Scholz, A. 2006, in Protostars and Planets V, in press (astro-ph/0603673)
Herbst, W., et al. 2002, A&A, 396, 513
Jayawardhana, R., Mohanty, S., & Basri, G. 2003, ApJ, 592, 282
Jayawardhana, R., et al. 1998, ApJ, 503, L79
———. 1999a, ApJ, 520, L41
———. 1999b, ApJ, 521, L129
———. 2001, ApJ, 550, L197
Johns, C., & Basri, G. 1995, AJ, 109, 2800
Kalas, P., Liu, M. C., & Matthews, B. C. 2004, Science, 303, 1990
Koenigl, A. 1991, ApJ, 370, L39
Köhler, R., & Petr-Gotzens, M. G. 2002, AJ, 124, 2899
Krist, J. E., et al. 2000, ApJ, 538, 793
Lawson, W. A., & Crause, L. A. 2005, MNRAS, 357, 1399
Lawson, W. A., Crause, L. A., Mamajek, E. E., & Feigelson, E. D. 2001, MNRAS, 321, 57
Lawson, W. A., Lyo, A. R., & Muzerolle, J. 2004, MNRAS, 351, L39
Low, F. J., Smith, P. S., Werner, M., Chen, C., Krause, V., Jura, M., & Hines, D. C. 2005, ApJ, 631, 1170
Luhman, K. L., & Steeghs, D. 2004, ApJ, 609, 917
Lyo, A.-R., Lawson, W. A., Feigelson, E. D., & Crause, L. A. 2004, MNRAS, 347, 246
Mamajek, E. E., Meyer, M. R., Hinz, P. M., Hoffmann, W. F., Cohen, M., & Hora, J. L. 2004, ApJ, 612, 496
Martin, E. L., & Ardila, D. R. 2001, AJ, 121, 2758
Megeath, S. T., Hartmann, L., Luhman, K. L., & Fazio, G. G. 2005, ApJ, 634, L113
Mohanty, S., Jayawardhana, R., & Barrado y Navascués, D. 2003, ApJ, 593, L109
Mohanty, S., Jayawardhana, R., & Basri, G. 2005, ApJ, 626, 498
Montes, D., Saar, S. H., Collier Cameron, A., & Unruh, Y. C. 1998, in ASP Conf. Ser. 154, The Tenth Cambridge Workshop on Cool Stars, Stellar Systems and the Sun, ed. R. A. Donahue, & J. A. Bookbinder (San Francisco: ASP), 1508
Muzerolle, J., Calvet, N., & Hartmann, L. 2001, ApJ, 550, 944
Muzerolle, J., et al. 2000, ApJ, 535, L47
Natta, A., et al. 2004, A&A, 424, 603
Rebull, L. M., Stauffer, J. R., Megeath, T., Hora, J., & Hartmann, L. 2005, BAAS, 37, 1477
Reipurth, B., Pedrosa, A., & Lago, M. T. V. T. 1996, A&AS, 120, 229
Richter, M. J., et al. 2002, ApJ, 572, L161
Scholz, A., & Jayawardhana, R. 2006, ApJ, 638, 1056
Scholz, A., Jayawardhana, R., & Brandeker, A. 2005, ApJ, 629, L41
Shu, F., et al. 1994, ApJ, 429, 781

Sicilia-Aguilar, A., Hartmann, L. W., Hernandez, J., Briceño, C., & Calvet, N. 2005, AJ, 130, 188
Stassun, K. G., et al. 1999, AJ, 117, 2941
Torres, G., et al. 2000, AJ, 120, 1410
———. 2003, AJ, 125, 825
Webb, R. A., et al. 1999, ApJ, 512, L63
White, R. J., & Basri, G. 2003, ApJ, 582, 1109
Wilner, D. J., Bourke, T. L., Wright, C. M., Jorgensen, J. K., van Dishoeck, E. F., & Wong, T. 2003, ApJ, 596, 597
Zuckerman, B., & Song, I. 2004, ARA&A, 42, 685